Toxicology Reports 14 (2025) 101856

Contents lists available at ScienceDirect

Toxicology Reports

journal homepage: www.elsevier.com/locate/toxrep

Gossypol enhances ponatinib's cytotoxicity against human hepatocellular carcinoma cells by involving cell cycle arrest, p-AKT/LC3II/p62, and Bcl2/caspase-3 pathways

Hadeel H. Elkattan [a,*], Alaa E. Elsisi [b], Naglaa M. El-Lakkany [a]

[a] Department of Pharmacology, Theodor Bilharz Research Institute, Warrak El-Hadar, Imbaba, Giza 12411, Egypt
[b] Department of Pharmacology and Toxicology, Faculty of Pharmacy, Tanta University, Tanta, Egypt

ARTICLE INFO

Handling Editor: Prof. L.H. Lash

Keywords:
Hepatocellular carcinoma
Ponatinib
Gossypol
Cell cycle arrest
Autophagy
Apoptosis

ABSTRACT

Despite significant breakthroughs in frontline cancer research and chemotherapy for hepatocellular carcinoma (HCC), many of the suggested drugs have high toxic side effects and resistance, limiting their clinical utility. Exploring potential therapeutic targets or novel combinations with fewer side effects is therefore crucial in combating this dreadful disease. The current study aims to use a novel combination of ponatinib and gossypol against the HepG2 cell line. Cell survival, FGF19/FGFR4, apoptotic and autophagic cell death, and synergistic drug interactions were assessed in response to increasing concentrations of ponatinib and/or gossypol treatment. Research revealed that ponatinib (1.25–40 μM) and gossypol (2.5–80 μM) reduced the viability of HepG2 cells in a way that was dependent on both time and dose. Ponatinib's anti-proliferation effectiveness was improved synergistically by gossypol and was associated with a rise in apoptotic cell death, cell cycle blockage during the G0/G1 phase, and suppression of the FGF19/FGFR4 axis. Furthermore, the ponatinib/gossypol combination lowered Bcl-2 and p-Akt while increasing active caspase-3, Beclin-1, p62, and LC3II. This combination, however, had no harm on normal hepatocytes. Overall, gossypol enhanced ponatinib's anticancer effects in HCC cells. Notably, this new combination appears to be potential adjuvant targeted chemotherapy, a discovery that warrants more clinical investigation, in the management of patients with HCC.

1. Introduction

Hepatocellular carcinoma (HCC) is the most common cancer among all primary liver cancers according to the World Health Organization, accounting for more than 70 % of cases. It is predicted to rank third among cancer-related deaths in 2020, with an annual increase in both occurrences and fatalities [1]. In clinical practice, the standard therapeutic options for HCC are surgery, chemotherapy, and radiotherapy [2]. Although substantial improvements many of the recommended drugs have extremely harmful adverse effects when used in combination with chemotherapy and front-line cancer research to treat HCC [3] and exhibit resistance, significantly limiting their use in the clinic.

HCC is hypothesized to be caused by abnormal activation of many intracellular cell proliferation and angiogenesis pathways including tyrosine kinase receptors as EGFR, VEGFR, PDGFR, FGFR, and others [4]. As a result, inhibiting the active site of a target kinase and preventing phosphorylation of intracellular targets that are frequently engaged in cell proliferation or angiogenesis [5,6]is crucial for cancer therapy. Sorafenib, a multi-kinase inhibitor, is currently the first-line therapy for HCC. However, its therapeutic efficacy is severely limited due to the development of drug resistance [7].

Natural products have shown to be excellent sources of innovative drug candidates. They make up over 80 % of anticancer medications used in clinical trials [8], and have multiple advantages such as non-toxicity, cost-effectiveness, availability, bioactivity, chemo-preventive potential, etc. [9]. Currently, numerous natural or mimicked natural products, such as paclitaxel, etoposide, irinotecan, and vincristine, have been approved for clinical usage as anticancer medications [10,11]. Among these, drugs that activate autophagy or apoptosis play a significant role. Furthermore, the development of specialized medications that inhibit cancer growth mechanisms, such as cell division acceleration by decreasing cell cycle proliferation, has emerged as a prospective necessity for developing cancer treatments [12].

* Corresponding author.
E-mail address: hadeelhesham94@gmail.com (H.H. Elkattan).

https://doi.org/10.1016/j.toxrep.2024.101856
Received 14 September 2024; Received in revised form 30 November 2024; Accepted 7 December 2024
Available online 11 December 2024

Consequently, identifying potential therapeutic targets or innovative combination strategies with fewer side effects is critical in combating this dreadful disease. Synergistic therapy targets many cancer pathways simultaneously and employs unique modes of action to prevent tumor drug resistance. In addition, it may lower medicine dosages and therapeutic adverse effects for patients [13]. Our earlier studies used a unique combination of the powerful multi-targeted kinase inhibitor, ponatinib, used to treat chronic myelogenous leukaemia, and gossypol, a yellow polyphenolic substance that was first discovered in cottonseed, demonstrated potent efficacy against solid Ehrlich carcinoma and colorectal cancer [14,15]. These studies, however, have certain limitations, as only colorectal cancer cell lines were tested for the synergistic impact of ponatinib and gossypol; therefore, this effect must be verified using other cell lines. Furthermore, more detailed parameters are needed to explore the autophagy/apoptosis interaction that underpins this synergistic effect. Additionally, we must evaluate the off-target effects of ponatinib, gossypol, or a combination of the two drugs on healthy hepatocytes.

Based on the foregoing, we hoped to look deeper into the potential mechanisms underlying this combination's synergistic effect. We investigated the antiproliferative properties of this innovative combination against the hepatocellular carcinoma HepG2 cell line. Furthermore, the distribution of apoptosis, the cell cycle profile, and the expression of proteins linked to autophagy were evaluated. In addition, the safety of ponatinib, gossypol, and their combination on hepatocytes was examined. Our study is the first to show that gossypol and ponatinib combination exhibited synergistic anti-tumor actions via impeding DNA synthesis and replication, inducing cell cycle arrest, boosting apoptotic and autophagic effects, and ultimately cytotoxicity to HCC cell lines, while remaining safe for normal hepatocytes. Overall, combining ponatinib and gossypol medication may be a powerful and safe clinical therapeutic strategy for HCC.

2. Materials and methods

2.1. Drugs and reagents

In this investigation, 100 mM stock solutions of ponatinib (943319–70–8; with purity ≥98 %) and gossypol-acetic acid (12542–36–8; with purity ~95 %) were acquired from BOC Science, BOCSCI Inc, 45–16 Ramsey Road Shirley New York, NY 11967, USA, and stored at −20 °C. Before use, the final dilutions were done immediately. Since the concentration of DMSO (analytical HPLC grade ~95 %) used in the experiment was less than 0.1 % (v/v), the cells were not harmed. Dulbecco's modified Eagle's medium (DMEM, Gibco, Life Technologies, America), fetal bovine serum (FBS, Gibco), 3-[4,5-dimethylthiazol-2-yl]-2,5-diphenyltetrazolium bromide (MTT), (5 mg/ml in PBS, Bio Basic Canada INC.), ab139418_ propidium iodide (PI) flow cytometry kit/BD (Abcam, Cambridge, UK), Annexin V-FITC and propidium iodide double-staining apoptosis detection kit (Biovision, USA), Radio immunoprecipitation assay (RIPA) buffer, PL005, Bio BASIC INC. (Marhham Ontario L3R 8T4 Canada)), RNeasy Mini Kit (Qiagen, Hilden, Germany), HERA SYBR® Green RT-qPCR Kit (WF1030300X), p-Akt (Catalogue No. 201–12–9003, Sun Red, China) and caspase-3 (Catalogue No. SRB-T-81642, Sun Red, China) were used. The ReadyPrepTM protein extraction kit (total protein) was provided by Bio-Rad Inc (Catalogue No. #163–2086). The Bradford Protein Assay Kit (SK3041) for quantitative protein analysis was supplied by Bio basic Inc. (Markham Ontario L3R 8T4 Canada). Polyacrylamide gels were performed using TGX Stain-Free™ FastCast™ Acrylamide Kit (SDS-PAGE), which was provided by Bio-Rad Laboratories inc (Catalogue No. # 161–0181). All chemicals used with high purity and analytical HPLC grade (>95 %).

2.2. Culture and cell lines

Human HCC cell line HepG2 (ATCC, HB-8065) and primary hepatocytes (ATCC, hepatic cell line BNL 1ME A.7 R.1; ATCC TIB-75) were purchased from VACSERA (Dokki, Giza, Egypt). HepG2 is a cell line with epithelial-like appearance that was obtained from the hepatocellular carcinoma of a 15-year-old, white youth male with liver cancer. While, non-malignant normal hepatocytes are epithelial cells obtained from the liver of a healthy mouse. Both HepG2 and hepatocytes were grown in 75-cm^2 flasks in DMEM supplemented with 10 % fetal bovine serum, 100 U/ml penicillin, and 100 μg/ml streptomycin and incubated at 37°C in a humidified incubator. (Vision Scientific Co., Ltd., Korea) with 95 % air and 5 % CO2. The media was continuously replenished every 3–4 days for the stock culture, and the cells were passaged when they reached 80 % confluence.

2.3. MTT assay

The viability of HepG2 and normal hepatocytes was tested with ponatinib, gossypol, and their combinations using the MTT assay. Based on the number of living cells, it measures how well mitochondrial dehydrogenases in viable cells can change the yellow tetrazolium salt MTT into blue formazan [16]. Briefly, HepG2 cells and hepatocytes (1×10^4 cells/well) were put into tissue culture plates with 96 wells (100 μl/well) and incubated for 24 h at 37 ℃ to generate a full monolayer sheet (80 % confluence). The culture media was subsequently changed with fresh medium containing a variety of concentrations of ponatinib (1.25 −40 μM), gossypol (2.5–80 μM), and in combinations (at a constant ratio of 1–2) dissolved at a final concentration of 0.1 % in vehicle DMSO. Each concentration was checked in triplicate on the same plate at the same time. After the plates were incubated at 37 ℃ for 24 and 48 h, the medium was removed and the cells were rinsed with PBS and 20 μl of MTT solution (5 mg/ml in PBS). They were then incubated for an additional 2–4 h at 37 ℃ in 5 % CO2. Each well received 100 μl of DMSO after the media was removed. A reader for microplates (mindray MR-96A) at 570 nm was utilized to calculate the cell lysates' optical density (OD). The results were shown as Mean ± SE. The cell viability percentage was estimated by multiplying the absorbance ratio between the compound-treated and untreated cells by 100. Using nonlinear regression analysis (GraphPad Software Instat, version 5; Inc., La Jolla, CA, USA), the IC_{50} (the dose of gossypol plus ponatinib needed to suppress cell growth by 50 %) was determined.

2.4. Analysis of drug interaction and the combination Index

CompuSyn (version 1.0.1) was used to examine the interaction between ponatinib (1.25–40 μM) and gossypol (2.5–80 μM) on HepG2 cells using the MTT test after 24 and 48 h. To display synergism (CI< 1), antagonistic effects (CI >1), additive effects (CI = 1), and dosage reduction index (DRI) for the medications taken together, the combination index (CI) was computed. When compared to the dose of each drug alone, the (DRI) indicates the number of folds of dose reduction that are allowed for each medication due to synergism. A DRI greater than one indicates a larger dose reduction for a given therapeutic effect [17–19]. After that, HepG2 cells were cultured for 24 h under usual conditions in 24-well plates at a density of 5×10^4 cells/well. After that, the cells in each well received a 48 h treatment with either ponatinib (IC_{50}), gossypol (IC_{50}), or a combination of the two. The cells were then taken out and prepared for the next measurements.

2.5. Morphological changes

Cells were evaluated under an inverted microscope for any preliminary morphological alterations indicative of cell toxicity, such as partial or total loss of monolayer, rounding, shrinkage, condensation, or cell granulation, after treatment with ponatinib (IC_{50}), gossypol (IC_{50}), or a combination of both. Morphological pictures of the cells were obtained using inverted phase contrast microscope (Reichert Jung, Nikon Eclipse TS200, Nikon) at a magnification of 200x and compared to

untreated control cells.

2.6. Cell cycle analysis

Using the ab139418_ propidium iodide (PI) flow cytometry kit/BD by the manufacturer's instructions, flow cytometry was utilized to examine the cell cycle. To summarize, ponatinib (IC_{50}), gossypol (IC_{50}), or both were applied to HepG2 cells (1×10^4 cells/well) for 48 h. After treatment, the cells were centrifuged at 1000xg, resuspended in 70 % ethanol, and fixed at 4 °C for an overnight period after being twice rinsed with ice-cold PBS. Subsequently, 40 μg/ml PI and 0.1 mg/ml RNase A were applied to the cells. The proportion of cells in the G0/G1, S, and G2/M phases was measured using a flow cytometer fitted with the FacsCalibur (BD Biosciences, USA) and examined using the Cell-Quest software (Becton Dickinson) due to the fact that DNA content differs amongst cells at different stages of the cell cycle [16]. HepG2 cells were used as a control group and their cell cycle was analyzed without any treatment.

2.7. Cell apoptosis analysis

The Annexin V-FITC/PI kit was used to quantify apoptosis according manufacturer's instructions. In summary, 5 x 10^5 HepG2 cells cultured on a 6-well plate were treated with ponatinib (IC_{50}), gossypol (IC_{50}), or a combination of the two for 48 h. After centrifugation, the cells were collected, twice washed in cold PBS, and then re-suspended in 500 μL of ice-cold annexin V-binding solution. This was followed by a combination of 5 μL of PI and 5 μL of Annexin V-FITC. Following a 15-minute dark incubation period, 400 μL of ice-cold annexin V-binding buffer was applied to the cells. Following incubation, flow cytometry utilizing BD Biosciences' FacsCalibur (USA) was used to identify apoptotic cells. The outcomes were shown using dot plot graphs.

2.8. Analysis of gene expressions by quantitative RT- PCR

Using a RNeasy Mini Kit (Qiagen, Hilden, Germany) and following the manufacturer's instructions, total RNA was extracted from cell pellets. Utilizing a nanodrop and absorbance measurements at 260 and 280 nm (1.8–2.0), the total RNA concentration and purity were assessed. Following the manufacturer's instructions, RT-PCR amplification and analysis were carried out in an optical 96-well plate (light cycler 480 II) using the HERA SYBR® Green RT-qPCR Kit (WF1030300X). The primers FGF19 and FGFR4 [20], Beclin-1 [21], Bcl-2, and glyceraldehyde-3-phosphate dehydrogenase (GAPDH, endogenous reference gene) [22] are shown in Table 1**.** The selected genes' relative expression was determined by the $2^{-\Delta\Delta Ct}$ method [23].

2.9. The Sandwich ELISA technique for protein analysis

The protein levels of both human p-AKT 1 (Catalogue No: 201–12–9003, Sun Red, China) and Caspase-3/CPP32 (Catalogue No: SRB-T-81642, Sun Red, China) in cell pellet lysate were determined via an enzyme-linked immunosorbent assay utilizing a double-antibody sandwich (ELISA) kit. Cysteinyl p-AKT or (Caspase-3/CPP32) was added to wells pre-coated with either human p-AKT1 or (Caspase-3/CPP32) monoclonal antibody. After incubation, p-AKT1 or (Caspase-3/CPP32) Biotin-tagged antibodies were added, then mixed with Streptavidin-HRP to form an immunological complex; the uncombined enzyme was then removed by repeating the incubation and washing steps. Then, Chromogen solution A and B were added, and the liquid's color changed from blue to yellow owing to the acid. The chroma of color was positively linked with the concentration of Human p-AKT1 or (Caspase-3/CPP32) in the sample. Total protein was quantified in each sample utilizing the Bradford test, using bovine serum albumin (BSA) as the standard.

Table 1
Sequences of primers for PCR analysis in real time.

Gene Name	Primer sequence
FGF19	**F**: 5′-GCACAGTTTG CTGGAGATCA−3′
	R: 5′-ATCTCCTCCTCGAAA GCACA−3
FGFR4	**F**: 5′-AGCACCCTACTGGACAC ACC−3′
	R: 5′-ACGCTCTCCATCACGAGACT−3′
Beclin−1	**F**: 5′ACAGAGCTCATGGAAGGGTCTA AGACGTCC−3′
	R: 5′-TACGAATTCT CATTTGTTATAAAATTGTG−3′
Bcl−2	**F**: 5′-ACTGGCTCTGTCTGAGTAAG−3′
	R: 5′-CCTGATGCTCTGGGTAAC−3′
GAPDH	**F**: 5′-GGGAAGGTGAAGGTCGGAGT−3′
	R: 5′-GGGGTCATTGATGGCAACA−3′

2.10. Analysis of protein expression via Western blot

To extract all of the cellular proteins, the cell pellets were treated with RIPA buffer, and the lysates were centrifuged at 10,000xg for 15 minutes at 4 °C. The Bradford protein assay kit (Bio-Rad) was used to determine the amount of protein present in the supernatants. Using immunoblotting analysis, the levels of LC3 II, P62, and β-actin (ACTB) were ascertained. In summary, each sample containing 20 μg of protein was heated to 95 °C for 8 minutes, then placed on a 12 % sodium dodecyl sulfate polyacrylamide gel (SDS-PAGE) and transferred into. polyvinylidene fluoride (PVDF) membranes. For two hours at room temperature, the membranes were blocked in tris-buffered saline containing 5 % nonfat milk and 0.1 % Tween-20 (TBST). Following an overnight incubation at 4 °C with primary antibodies against LC3 II and P62 and α-actin (ACTB) at a dilution of 1:1000, the membranes were three times washed with TSBT. The membranes were then cleaned and exposed to a 1:1000 dilution of the secondary antibody conjugated with HRP. The ClarityTM Western ECL substrate (Bio-Rad cat#170–5060) was added to the blot in accordance with the manufacturer's instructions to enhance chemiluminescence and visualize protein bands. Using protein normalization, image analysis software was employed on the ChemiDoc MP imager to determine the band intensity of the target proteins in comparison to the housekeeping protein, β-actin, as a control sample.

2.11. Statistical analysis

The data is shown as Mean ± SEM. Using SPSS, software package version 16.0 (Chicago, IL, USA), a one-way ANOVA test and Tukey's *post hoc* test were used to determine the statistical difference between the mean values of the various groups. A *P* value of less than 0.05 were considered statistically significant.

3. Results

3.1. Gossypol enhances the cytotoxic effect of ponatinib in HepG2 cells

Using the MTT assay, the impact of gossypol on ponatinib's cytotoxicity was initially identified. Ponatinib (1.25–40 μM) and gossypol (2.5–80 μM) both decreased cell viability in a way that was dependent on time and dose (Fig. 1A and B). Based on the fitted survival curves, the half-maximal inhibitory concentrations (IC_{50}) of gossypol and ponatinib were determined. The IC_{50}s values were 8.38 and 21.35 μM, respectively after 24 h and 5.15 and 13.32 μM, respectively after 48 h. More importantly, co-treatment of HepG2 cells with ponatinib and gossypol resulted in 2.2-fold and 2.5-fold reductions in IC_{50} (3.79 and 2.04 μM) after 24 h and 48 h, respectively, in contrast to the cells treated with ponatinib **(**Fig. 1**C and D)**, indicating excellent augmenting anti-HCC activity.

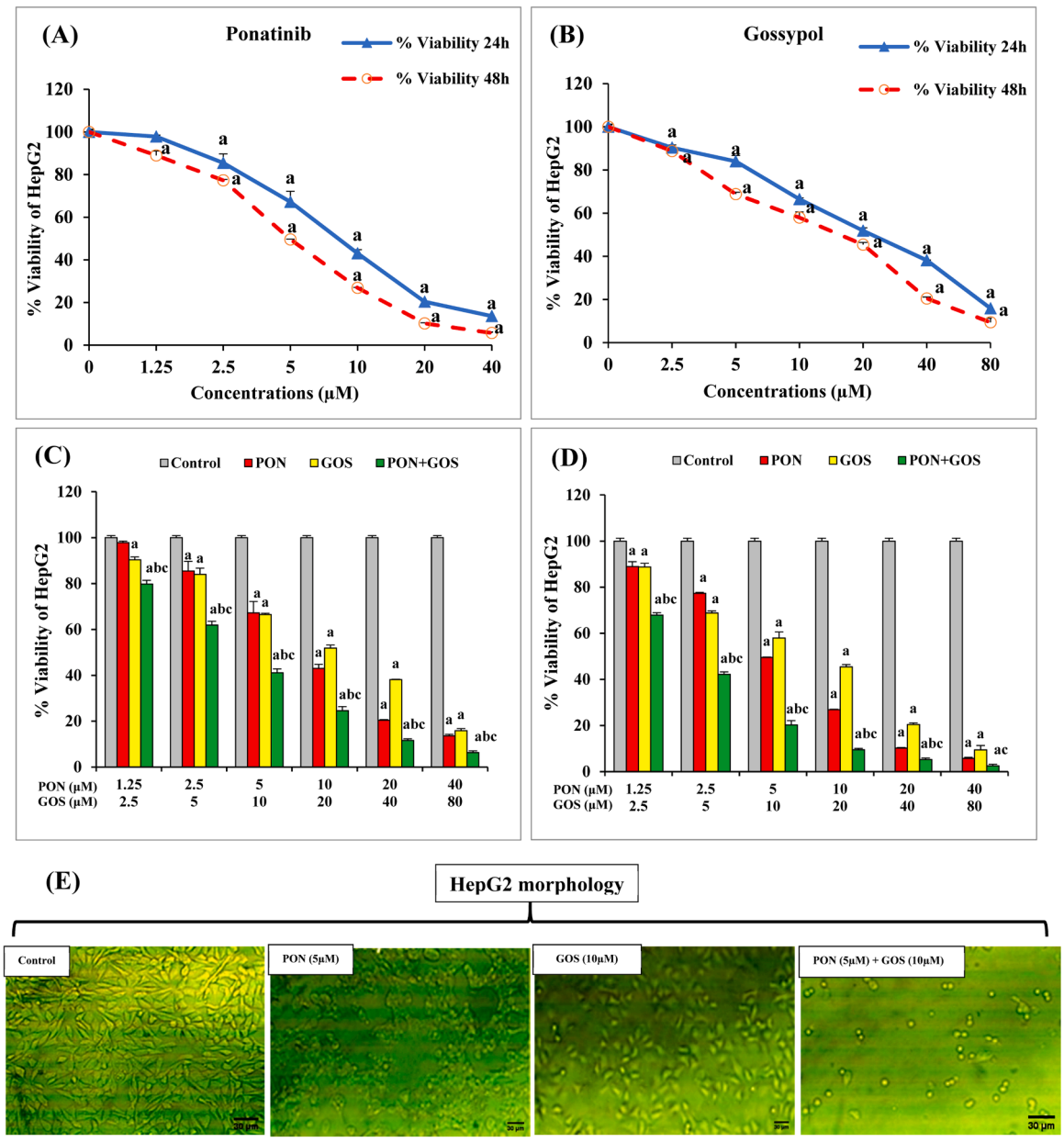

Fig. 1. The effect of ponatinib (1.25 −40 µM) and gossypol (2.5–80 µM) alone **(A and B)** and their combination **(C and D)** at 1: 2 ratios on the viability of HepG2 cells after 24 and 48 h, respectively, using the MTT assay. The cell viability percentage was calculated by multiplying the absorbance ratio between the compound-treated cell culture and the untreated control by 100. Data are presented as Mean ± SEM (n = 3) and analyzed by one-way ANOVA test followed by a Tukey's *post hoc* test. **(E)** The effect of ponatinib and/or gossypol on HepG2 morphological alterations after 48 h. Morphological pictures of the cells were obtained using an inverted phase contrast microscope (Reichert Jung, Nikon Eclipse TS200, Nikon) at a magnification of 200x. PON: ponatinib, GOS: gossypol. [a, b, c] Significantly different from untreated control, PON and GOS groups, respectively, at $P < 0.05$.

3.2. Effect of ponatinib/gossypol combination on the morphological changes of HepG2 cells

After 48 h, a preliminary morphological assay was used to evaluate the morphological effects of ponatinib (IC_{50}) and gossypol (IC_{50}) in HepG2 cells, and the results were examined under an inverted phase contrast microscope, as shown in Fig. 1E. The control HepG2 cells formed an 80 % confluent monolayer sheet that appeared intact. Treatment of cells with ponatinib (IC_{50}) or gossypol (IC_{50}) alone resulted in a loss of normal shape, with cells appearing smaller in size, shrunken and rounded, swelling, and with low density. Notably, co-treatment with ponatinib and gossypol revealed complete monolayer destruction, with cell appearing spare and fully separated from the plates' surface, loss of cell adhesion capacity, and a reduction in cell number reaching roughly half that of ponatinib or gossypol-treated cells, indicating that the ponatinib/gossypol combination considerably inhibits HepG2 cell proliferation over either alone.

3.3. Safety of ponatinib/gossypol combination on hepatocyte cell growth and viability

The concentrations of ponatinib and/or gossypol used in our study were shown to be safe, with only mild toxicity at higher concentrations. Adding ponatinib (1.25 −40 µM) and gossypol (2.5 −80 µM) alone to the culture medium of primary hepatocytes resulted in about 99 −77 % and 99 −76 % viability, respectively, after 48 h. The addition of combined ponatinib/gossypol to hepatocyte culture media resulted in cell viability ranging from 98 % to 68 % after 48 h, as illustrated

morphologically in Fig. 2**A** and graphically **in** 2**B.**

3.4. Synergistic interaction between ponatinib and gossypol in HepG2 cells

Fig. 3 depicts the combination indices (CIs) obtained after treating HepG2 cells with various concentrations of the two drugs, as well as the pattern of their interaction. The CI values in HepG2 ranged from 0.74 to 1.06 after 24 h and from 0.62 to 0.91 after 48 h, indicating superior synergism when HepG2 cells were treated for 48 h rather than 24 h. When compared to the dose of each drug alone, (DRI) reflects the number of folds of dose reduction that are allowed for each drug due to synergism. A DRI greater than one suggests a greater dose reduction for a given therapeutic benefit [17–19]. The combination also demonstrated that the DRI values for ponatinib were always greater than one at any two-drug combination point. Furthermore, the combination of 5 μM ponatinib and 10 μM gossypol, which represented approximately their IC_{50} values in HepG2, inhibited growth by 79 % with CI = 0.62 (Table 2), demonstrating the greatest synergism with the higher DRI of ponatinib by 2.66-fold. Based on these findings, the mechanisms behind ponatinib and gossypol synergy on HepG2 cells were studied, including growth inhibition, autophagy-associated proteins, apoptosis, cell cycle arrest, and proliferation.

3.5. Ponatinib and gossypol combination induced cell cycle arrest in HepG2 cells

Cytotoxic anticancer drugs work by inhibiting cell growth at certain cell cycle checkpoints. When these phases are suppressed, cell growth halts. Flow cytometry is used in cell cycle investigations to distinguish between cells at various phases of the cell cycle. Fig. 4 displays graphs of fractional DNA content (PI fluorescence, X axis) and cell counts (Y axis)

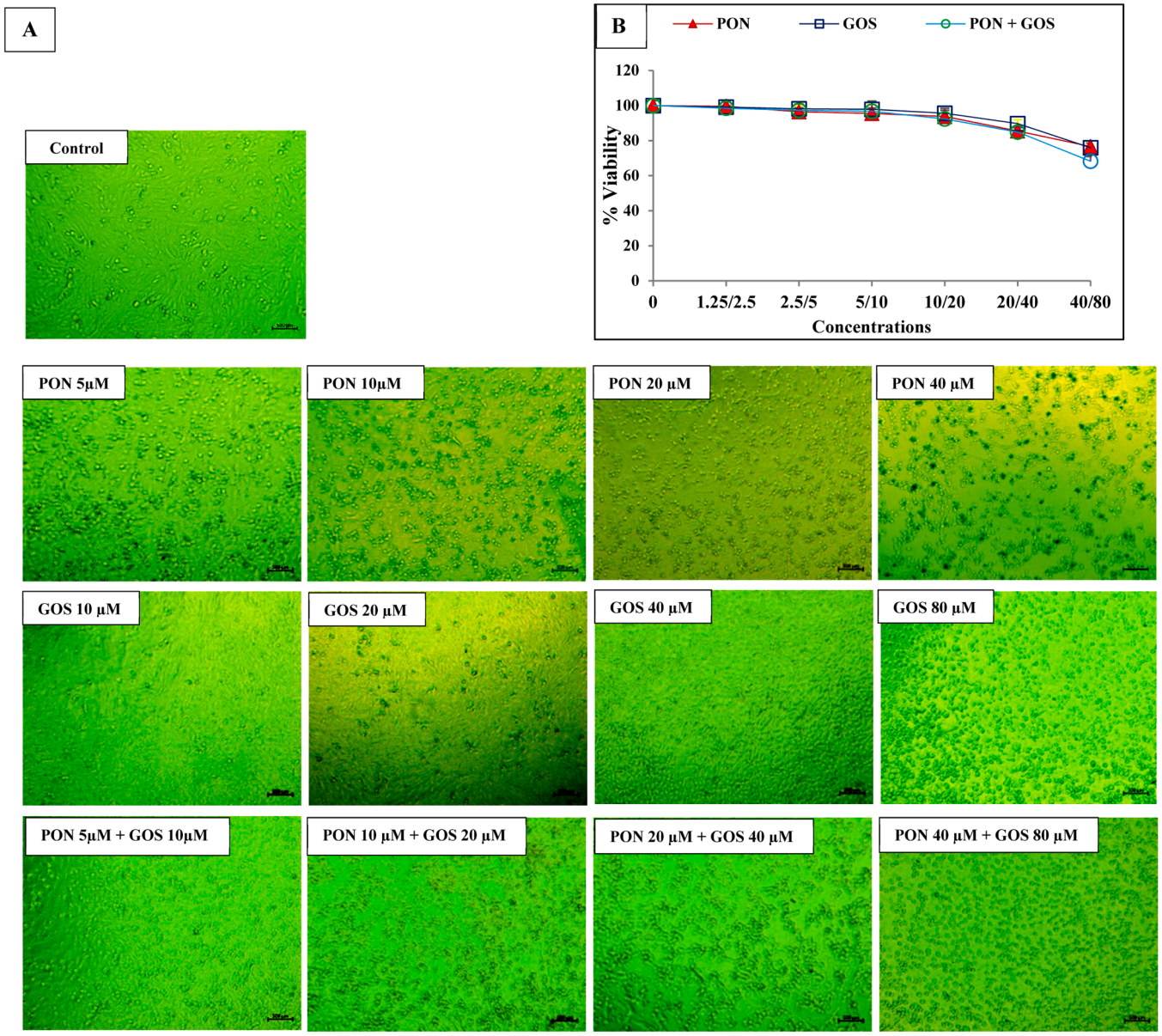

Fig. 2. The effect of ponatinib (1.25 −40 μM) and gossypol (2.5–80 μM) alone or in combination at 1: 2 ratios on the morphological alterations of primary hepatocytes after 48 h **(A)**. Morphological pictures of the cells were obtained using an inverted phase contrast microscope (Reichert Jung, Nikon Eclipse TS200, Nikon) at a magnification of 200x. **(B)** The effect of ponatinib and/or gossypol on the % viability of normal hepatocyte after 48 h, using the MTT assay. The cell viability percentage was calculated by multiplying the absorbance ratio between the compound-treated cell culture and the untreated control by 100. Data are presented as Mean ± SEM (n = 3) and analyzed by one-way ANOVA test followed by a Tukey's *post hoc* test. PON: ponatinib, GOS: gossypol.

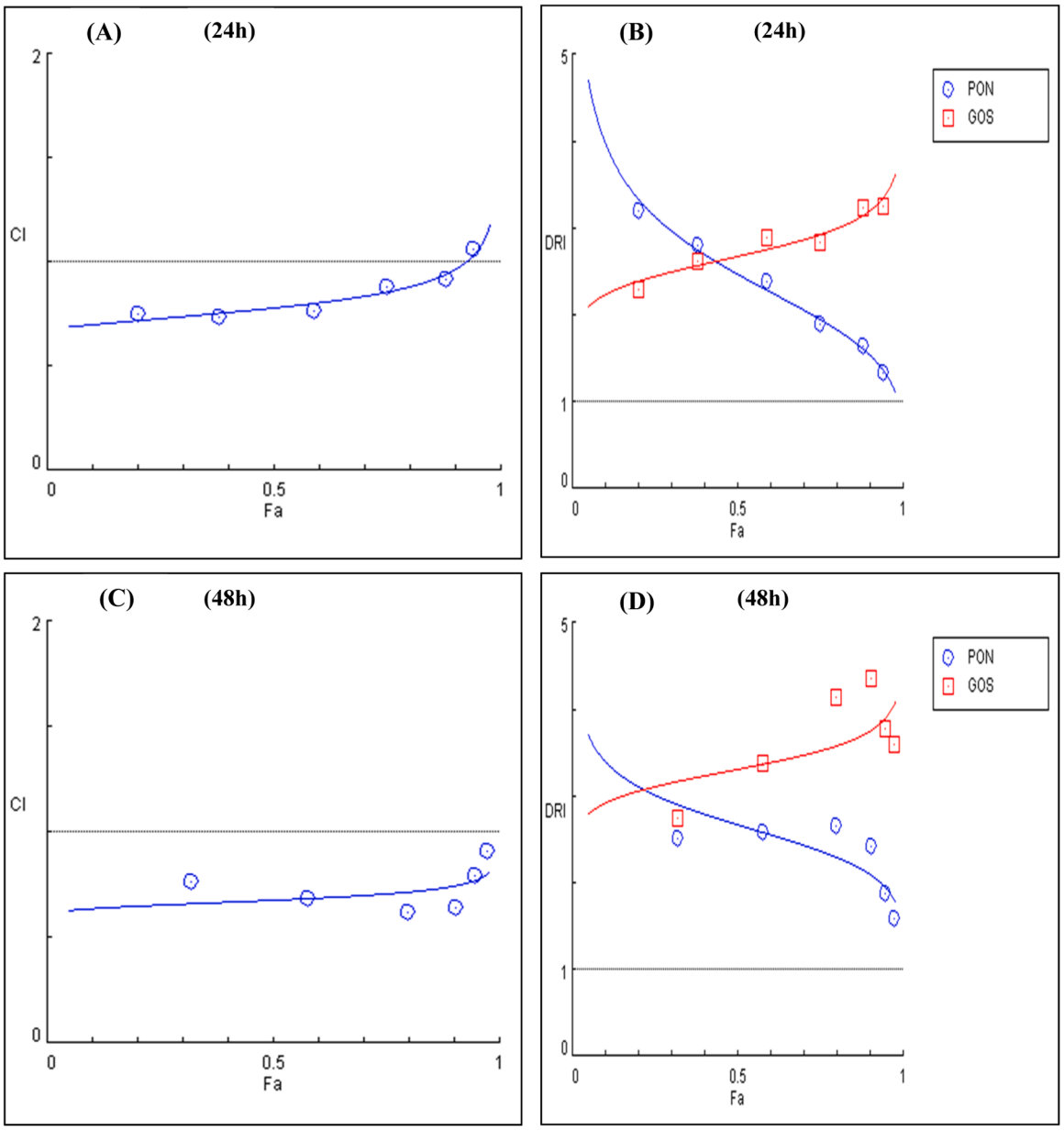

Fig. 3. Combination **(A and C)** and dose reduction **(B and D)** index plots of ponatinib combined with gossypol at a constant ratio (1:2) in HepG2 at 24 h and 48 h, respectively. CI < 1, CI = 1, and CI > 1 represented synergism, additive effect, and antagonism, respectively. The CI is calculated as (dA/DA) + (dB/DB), where dA and dB are the concentrations of PON and GOS together, and DA and DB are the concentrations of PON or GOS that induce the same effect alone. The computer software CompuSyn (version 1.0.1) was used to calculate the combined drugs' CI, DRI, and Fa. PON: Ponatinib, GOS: Gossypol, CI: Combination Index, DRI: Dose reduction index, Fa: Fraction affected.

of HepG2 cells at various cell cycle stages (G0/G1, S, and G2/M) after 48 h of incubation with IC_{50} of ponatinib (5 μM), gosypol (10 μM), or both. HepG2 cells treated with ponatinib accumulated in the G0/G1 phase, increasing ($P > 0.05$) from 44 % ± 0.80 in untreated cells to 47 % ± 0.84 in treated cells, with a concurrent significantly increase in the percentage of cells in S phase ($P < 0.05$) (from 39 % ± 0.36 in untreated cells to 43 % ± 1.10 in treated cells) **(**Fig. 4**B and E)**. Likewise, gossypol has been shown to promote cell accumulation in the S phase ($P < 0.05$), which is 46 % ± 0.84 higher than the control (39 % ± 0.36), accompanied by a decrease in the proportion of cells in G0/G1 and G2/M phases **(**Fig. 4**C and E)**. However, treating HepG2 cells with ponatinib and gossypol in combination resulted in alterations in cell distribution during the G0/G1 and S phases. Compared to control and ponatinib or gossypol alone, the proportion of cells in G0/G1-phase increased dramatically ($P < 0.05$) from 44 % ± 0.80–52 % ± 0.87, resulting in near-complete G0/G1 arrest and a significant decrease ($P < 0.05$) in the proportion of cells in S-phase **(**Fig. 4**E)**, indicating a lack of growth and DNA synthesis.

3.6. Gossypol enhances the anti-proliferative activity of ponatinib in HepG2 cells

When HepG2 cells were treated with ponatinib (5 μM) and gossypol (10 μM) separately, they induced a significant ($P < 0.05$) reduction in the expression of genes FGF19 by 83 % and 48 %, respectively, and FGFR4 by 64 % and 34 %, respectively, after 48 h, when compared to the untreated control **(**Fig. 5**)**. Furthermore, the combination of ponatinib (5 μM)/gossypol (10 μM) reduced significantly ($P < 0.05$) both FGF19 and FGFR4 gene expression by 99 % and 97 %, respectively. When compared to the ponatinib alone group, this combination caused a

Table 2
Indexes for combination and dose reduction when ponatinib is added to gossypol in HepG2 cells for 24 and 48 h.

PON (μM)	GOS (μM)	Fa		CI		DRI PON	
		24 h	48 h	24 h	48 h	24 h	48 h
40	80	0.94	0.98	1.06	0.91	1.32	1.58
20	40	0.88	0.95	0.92	0.79	1.65	1.88
10	20	0.75	0.91	0.88	0.64	1.89	2.42
5	10	0.59	0.79	0.77	0.62	2.39	2.66
2.5	5	0.38	0.58	0.74	0.68	2.80	2.59
1.25	2.5	0.2	0.32	0.75	0.76	3.20	2.51

HepG2 cells were treated with the combination of ponatinib and gossypol at the doses indicated for 24 and 48 h. CI < 1, CI= 1, and CI > 1 indicated synergism, additive effect, and antagonism, respectively. The CI= (dA/DA) + (dB/DB), where dA and dB are the concentrations of PON and GOS in combination, whereas, DA and DB are the concentrations of PON or GOS, respectively, which produce the same effect alone. The computer software CompuSyn (version 1.0.1) was used for the determination of CI, DRI and Fa for the drugs in combination. PON: ponatinib, GOS: gossypol, CI: combination index, DRI PON: Dose reduction index of ponatinib, Fa: fraction affected.

greater ($P < 0.05$) and synergistic reduction in both FGF19 and FGFR4 gene expression by 94 % and 92 %, respectively.

3.7. Gossypol enhances the apoptotic activity of ponatinib in HepG2 cells

One of the main causes of cell death and growth inhibition is cellular apoptosis [24]. It is possible to determine if uncontrollably occurring necrosis or programmed apoptosis is the source of cell death by doing the double-staining experiment with PI and Annexin V-FITC. The differentiation of live cells, early apoptotic cells, late apoptotic cells, and necrotic cells is made possible by dual labeling for Annexin-V and PI. To confirm the quantitative efficiency of apoptosis induction and to ascertain whether the synergistic cell growth inhibition by ponatinib/gossypol combination accompanied the induction of apoptosis in HepG2 cells, Annexin V-FITC and PI were used to stain ponatinib, gossypol, ponatinib/gossypol-treated HepG2 cells, and untreated cells.

Based on staining and phase (viable: PI and Annexin-V negative, early apoptosis: PI negative and Annexin-V positive, late apoptosis: PI and Annexin-V positive, necrotic: PI positive and Annexin-V negative), flow cytometry was used to distinguish the cells. Two stages of apoptosis are distinguished: early-stage apoptosis, which is displayed in the FACS histograms' lower right quadrants, and late-stage apoptosis/necrosis, which is displayed in the upper right quadrants. The findings demonstrated that either ponatinib or gossypol alone to HepG2 cells for 48 h caused a considerable amount of early and late-stage apoptosis in the cells **(**Fig. 6**B and C)**, with a higher percentage of cells undergoing early-stage apoptosis than late-stage apoptosis/necrosis. On the other hand, more cells were in late-stage apoptosis/necrosis than early-stage apoptosis when HepG2 cells were treated with both ponatinib and gossypol for 48 h **(**Fig. 6**D)**. The combination of ponatinib (5 μM) and gossypol (10 μM) resulted in a larger ($P < 0.05$) rise in late apoptosis/necrosis as compared to the ponatinib alone group, with a percent increase ($P < 0.05$) of around > 2.00-fold **(**Fig. 6**E)**.

A series of caspase cleavage and activation events are indicative of apoptosis [25]. There are two types of apoptosis mechanisms: caspase-dependent and caspase-independent. To fully explore the apoptosis induction pathway, we looked at the expression levels of the Bcl-2 gene and the caspase-3 protein in HepG2 cells **(**Fig. 6**F and G)**. Treatment with ponatinib (5 μM) and gossypol (10 μM) individually for 48 h caused a significant ($P < 0.05$) reduction in Bcl-2 gene expression by 84 % and 86 %, respectively, and a significant ($P < 0.05$) increase in caspase-3 protein level by 1.65 and 1.73-fold. Meanwhile, the combination of ponatinib (5 μM) and gossypol (10 μM) caused the best ($P < 0.05$) reduction in Bcl-2 gene expression associated with a higher increase in caspase-3 protein expression than either agent alone, with a marked ($P < 0.05$) difference by about 87 % and 1.96-fold, respectively, when compared to the ponatinib group alone. These findings suggest that apoptosis is caused in HepG2 cells via both intrinsic and extrinsic routes, with mitochondria and Bcl-2 family members linked to ponatinib/gossypol-induced cell death.

3.8. Gossypol enhances the autophagic activity of ponatinib in HepG2 cells

When HepG2 cells were treated for 48 h with ponatinib (5 μM) or gossypol (10 μM), they caused a substantial ($P < 0.05$) increase in Beclin-1 gene expression in the ponatinib group, but an apparent increase in gossypol by 4.53 and 3.04-fold, respectively when compared to the control **(**Fig. 7**)**. This was associated with a substantial drop ($P < 0.05$) in p-Akt protein levels of 20 % and 16 %, respectively, and a rise ($P < 0.05$) in LC3II protein levels by 2.00 and 1.80-fold. Furthermore, gossypol caused a 3.44-fold rise in p62 protein levels, but ponatinib demonstrated a marginally non-significant increase ($P > 0.05$). The combination of ponatinib (5 μM) and gossypol (10 μM) led to the most notable ($P < 0.05$) increase in Beclin-1 gene expression and the greatest decrease in p-Akt protein level. This was associated with an increase in LC3II and P62 protein levels, with a significant ($P < 0.05$) difference of about 10.33-fold, 46 %, 2.73-fold and 5.01-fold, respectively, when compared to control, and with a marked ($P < 0.05$) difference by about 2.28-fold, 32 %, 1.37-fold, and 4.48-fold, respectively, when compared to the ponatinib group alone **(**Fig. 7**)**.

4. Discussion

Worldwide, liver cancer is the leading cause of mortality from cancer, and the World Health Organization estimates that it will kill approximately one million people by 2030 [26] Despite the fact that HCC has a variety of treatment options, the 5-year survival rate remains low [27]. Chemotherapy is one of the most commonly used HCC treatment options, but its high cytotoxicity and poor selectivity have the potential to seriously harm healthy cells [28]. Exploration of potential therapeutic targets or novel combination strategies is therefore urgently required. Combination therapy is used to treat a wide range of cancers with complex pathology around the world, and it has the potential to significantly reduce drug toxicity and chemo-resistance while increasing efficacy and providing selective synergism against a target [29]. We previously demonstrated potent efficacy against solid Ehrlich carcinoma and colorectal cancer using a novel combination of ponatinib, a potent multi-targeted kinase inhibitor used to treat leukemia, and gossypol, an extract of yellow polyphenols that were first discovered in cottonseed [14,15]. This novel therapeutic strategy seeks to improve ponatinib efficacy while lowering major side effects such an elevated risk of vascular occlusive disease and heart failure. In the current study, we anticipated to investigate its effects on another type of cancer cell line, such as HepG2, as well as the potential mechanisms underlying this combination's synergistic effect by examining expression of proteins linked to autophagy, cell viability, and dispersion of the cell cycle profile. Also, since combination treatment may damage non-cancerous cells, it was imperative to look into the cytotoxic effect of ponatinib/gossypol combination on normal hepatocytes.

The findings unequivocally showed that gossypol significantly reinforces the anti-tumor effects of ponatinib, with co-treatment of HepG2 cells with ponatinib/gossypol at a constant ratio of 1–2 consistently demonstrating a greater inhibition of cell proliferation, as evidenced by a ~ 2-fold reduction in IC_{50}s (3.79 μM & 2.04 μM) after 24 h and 48 h, respectively, as compared to IC_{50} of ponatinib-treated cells (8.38 μM & 5.15 μM, respectively). Ponatinib and gossypol together had a synergistic effect on cancer cell proliferation in HepG2 cells, as indicated by CI and DRI values at 24 and 48 hours, according to the isobologram analysis for two-drug interactions. A synergistic impact was evident at low IC_{50} concentrations, as most tested concentrations had CI values < 1.

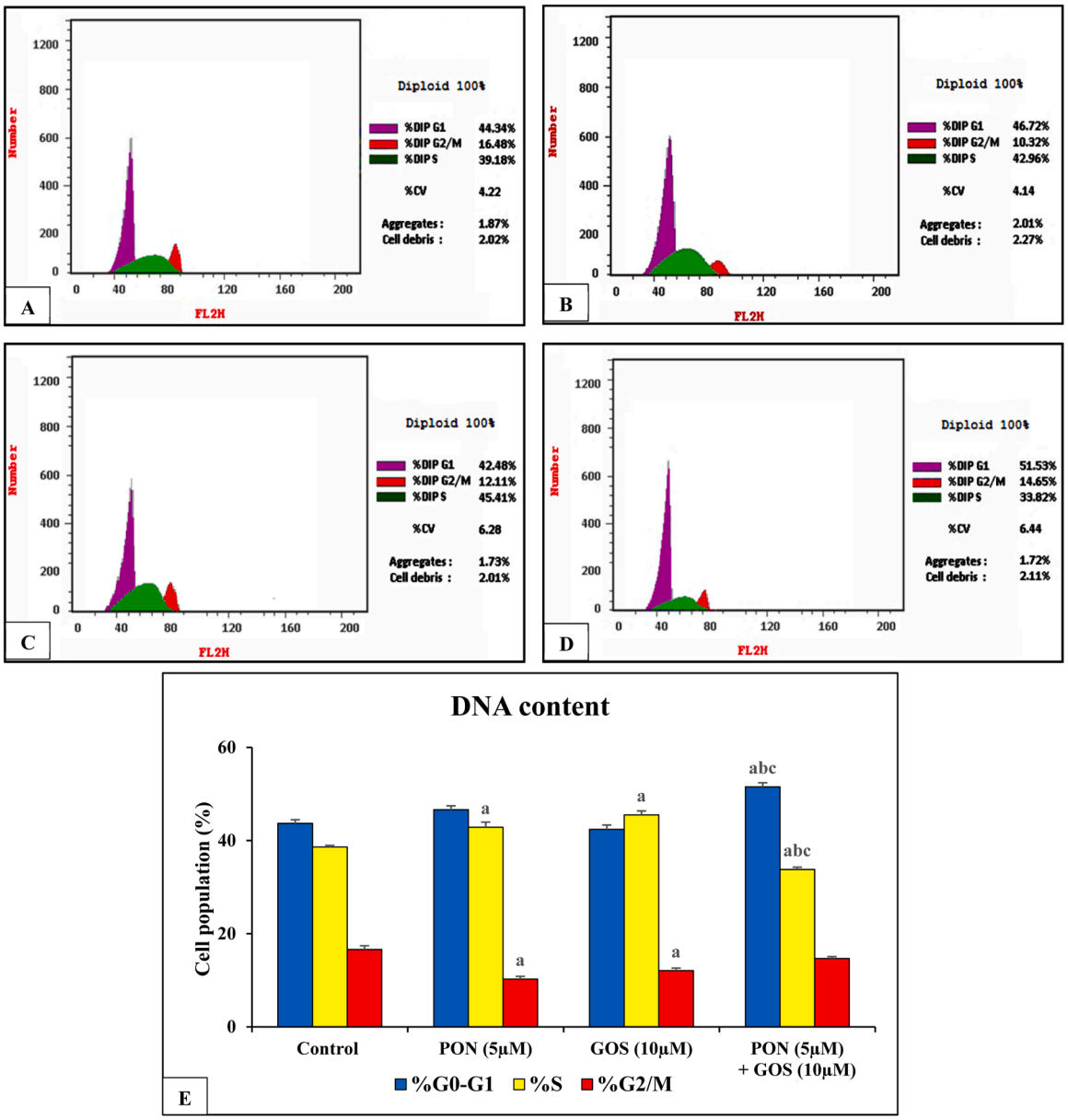

Fig. 4. Ponatinib and gossypol combination induced cell cycle arrest at G0/G1 in HepG2 cells. Cell cycle distribution of HepG2 cells was analyzed by flow cytometry at different phases after 48 hours in **(A)** untreated control, **(B)** PON IC_{50}, **(C)** GOS IC_{50}, and **(D)** PON IC_{50} + GOS IC_{50}. **(E)** Cell cycle distribution of HepG2 cells at different phases is represented as a histogram. Data are presented as Mean ± SEM (n = 3) and analyzed by one-way ANOVA test followed by a Tukey's *post hoc* test. IC_{50}: the dose of ponatinib and gossypol required to suppress cell growth by 50 % and was determined using nonlinear regression analysis (GraphPad Software Instat, version 5; Inc., La Jolla, CA, USA). PON: ponatinib, GOS: gossypol. [a, b, c] Significantly different from the untreated control, PON and GOS groups, respectively at P <0.05.

Since the DRI values were greater than 1, we were able to mostly prevent ponatinib toxicity by mixing gossypol and ponatinib, which was especially beneficial at low dosages.

Cell cycle and apoptosis of ponatinib/gossypol-treated HepG2 cells were next examined. Cell growth and proliferation can be prevented in one of two ways: by inducing apoptosis or by arresting the cell cycle. As a result, it is claimed that combining molecular targeted drugs with agents that cause DNA damage or cell cycle arrest may boost anti-tumor efficacy [7]. Apoptosis is caused by many anti-tumor and DNA-damaging drugs that interfere with the cell cycle in the G1/S or S phase to stop improper DNA replication, or in the G2/M phase to prevent mitosis with damaged DNA [30]. In this investigation, we employed flow cytometry to examine if ponatinib, gossypol, or their combinations altered the cell cycle of HepG2 cells. Combining ponatinib and gossypol treatment substantially improved anti-tumor effects on HCC cell lines by stopping cells in the G0/G1 phase, which was associated with increased apoptotic and necrotic cells versus each drug alone, as indicated by cycle analysis and V-FITC/PI staining, implying that they impede DNA synthesis and replication. Previous studies reported that ponatinib stimulated cell cycle arrest at G1 in liver cancer [31,32], while gossypol arrest the cell cycle at G1 phase in gastric cancer [33]. In HepG2 cells, Bcl-2, an antiapoptotic protein, and caspase-3, a key protein regulator of apoptosis, were also evaluated. Bcl-2 family proteins are well-known for their involvement in the mitochondrial apoptotic pathway [34]. Caspase-3 is a major apoptotic executive caspase that activates in a cascade during apoptosis via proteolytic cleavage of caspase 9 [25]. After 48 h of treatment, the ponatinib/gossypol combination lowered Bcl-2 protein levels while raising active caspase-3 protein levels, indicating enhanced apoptosis compared to the individual drugs. Gossypol increases caspase-3 while decreasing Bcl-2 in BxPC-3 and MIA PaCa-2

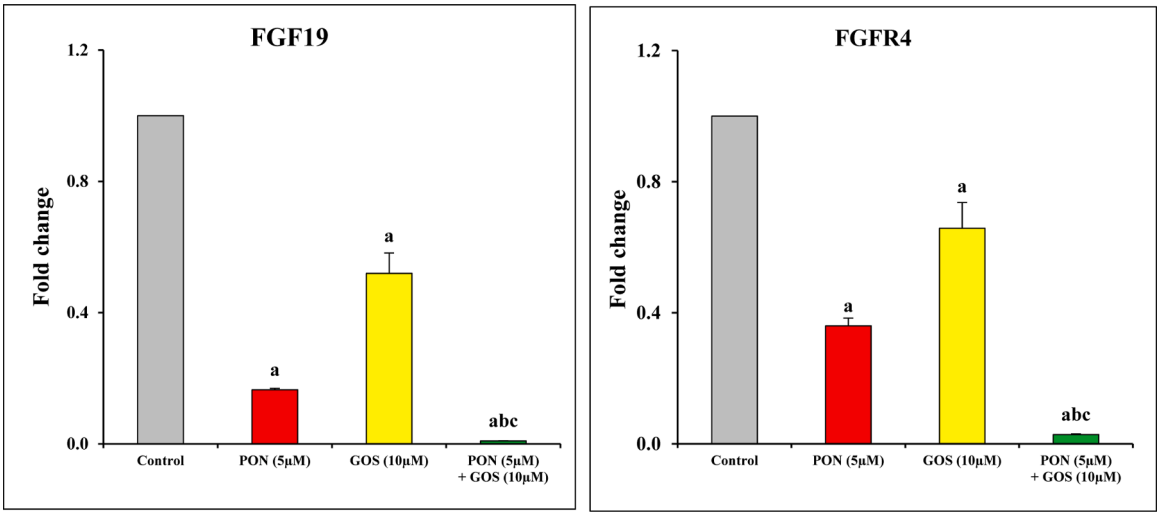

Fig. 5. The effect of ponatinib alone and in combination with gossypol on FGF19/FGFR4 axis in HepG2 cells after 48 h. Data are presented as Mean ± SEM (n = 3) and analyzed by one-way ANOVA test followed by a Tukey's *post hoc* test. PON: ponatinib, GOS: gossypol. [a, b, c] Significantly different from the untreated control, PON and GOS groups, respectively at P <0.05.

cells [35], HT-29 cells [36], MCF-7 cells [37], and AtT20 cells [38]. Similarly, ponatinib inhibited Bcl-2 expression in SK-Hep-1 and SNU-423 cells [31] and TccY/Sr cells [39] suggesting that the mitochondrial apoptotic pathway is connected to ponatinib-induced apoptosis in a concentration-dependent manner.

The observed apoptosis caused by combination therapy agreed with the cytotoxicity testing and preliminary morphology results, where co-treatment with ponatinib and gossypol revealed decreased cell viability/proliferation, complete monolayer destruction, with cells appearing spare and detached completely from the surface of the plates, loss of cell adhesion capacity, and a cell number reduction reaching roughly half that of ponatinib or gossypol-treated cells, indicating that the ponatinib/gossypol combination significantly inhibits HepG2 cell proliferation over either drug alone. Ponatinib/gossypol's anti-proliferative activity matched with synergistic inhibition of the FGF19/FGFR4 axis, resulting in a decrease in cell viability in HepG2, which is associated with an increase in many types of cell death (apoptosis and autophagy). This is consistent with our recent results [14], which indicated that ponatinib/gossypol was effective on CRC cell lines by targeting FGF19/FGFR4. FGF19 selectively binds to FGFR4, and abnormal FGF19 signaling is translocated into tumor cells via a variety of oncogenic routes, resulting in tumor-promoting activity, with FGF19-FGFR4 binding activating downstream signaling cascades such as PI3K/AKT, apoptosis, and autophagy [40]. Notably, in this study, FGFR4 deletion was linked to lower Bcl-2, higher caspase-3, and increased apoptosis. It was discovered that the induction of apoptosis by FGFR depletion was FLIP- and Bax-dependent. This led to the activation of caspase 8, which in turn promoted the release of Bax-mediated cytochrome c and activation of caspase 9, which in turn activated the executioner caspases 3 and 7, ultimately resulting in apoptosis [41]. Additionally, Turkington et al. [42] revealed that FGFR4 controls apoptosis via altering the anti-apoptotic proteins cellular FLICE-inhibitory protein (c-FLIP) and Bcl2. In another study, FGFR4 interaction with the βKlotho (KLB) co-receptor, a metabolic regulator altered in hepatic malignancies, was demonstrated to decrease cell proliferation and cause caspase-3-dependent death in hepatomas via lowering AKT and m-TOR activity [43]. Combining these data, we propose that ponatinib and gossypol's apoptotic effects may also be attributed to their inhibitory activity on FGFR, in addition to the apoptotic effects mediated by decreased Bcl-2 and elevated caspase-3. However, more research is needed to fully understand the most likely mechanism.

In addition to apoptosis, this study looked into autophagy as a potential mechanism for cancer therapy. Autophagy can either direct or collaborate with apoptosis to trigger cell death [44], where moderate autophagy helps cells survive by maintaining cell homeostasis, but excessive autophagy destroys essential cellular components and functions, eventually leading to cell death [45]. Intriguing research explored that blocking autophagy in HCC can increase apoptosis and decrease tumor cell growth rate when exposed to photothermal therapy [46]. Autophagy and apoptosis interact in both normal and malignant cells, as well as in other illnesses, although their importance in HCC has been overlooked in some studies [47]. Thus, our results may provide insight into how autophagy-apoptosis crosstalk functions in HCC.

Caspases were found to be involved in regulating the interaction between autophagy and apoptosis [48]. Several pro-apoptosis mechanisms can activate caspases, which then cleave and degrade key autophagic proteins such as Beclin-1 and p62, promoting crosstalk between apoptotic and autophagic pathways [49]. P-Akt, Beclin-1, LC3II, and p62 are autophagy-regulating proteins, with p-Akt overexpression in cancer leading to phosphorylation of Beclin-1, which is required for autophagy initiation and autophagosome formation [50]. Herein, following ponatinib/gossypol treatment, p-Akt protein levels decreased while Beclin-1 expression increased. [36,51,52] state that both ponatinib and gossypol promote autophagy. Apoptosis and autophagy are two modes of cell death with intricate connections [53]. Beclin-1, a key autophagy-inducing protein, is inhibited by Bcl-2 or Bcl-xL [54,55]. Lowering Bcl-2 improves Beclin-1 accessibility, boosting autophagy [56]. Gossypol, a BH3 mimic, binds to anti-apoptotic Bcl-2 proteins [57], disrupting Bcl-2 and Beclin-1 interactions at the endoplasmic reticulum, decreasing Bcl-2 levels, and increasing Beclin-1 expression in cancer cells by inducing the Beclin-1 Atg5-dependent autophagic [58], thus regulating apoptosis and autophagy [59,60]. Beclin-1 regulates cell death processes like apoptosis and autophagy by binding Bcl-2 family members [61,62], activating pro-apoptotic proteins Bax and Bak, releasing cytochrome c, and activating caspase-9 and −3 [63]. Overall, our study suggests that the modification of Bcl-2 and Beclin-1 significantly regulates the interaction between autophagy and apoptosis, though further research is needed to understand the exact mechanism.

In addition, changes in LC3-II and p62 protein expression indicate autophagy initiation. Cytosolic LC3-I attaches to phosphatidylethanolamine on autophagosome surfaces, generating LC3-II [64]. P62, an autophagy negative regulator, can also create autophagosomes by interacting directly with the target protein LC3 [65,66]. Ponatinib was shown to increase LC3-II protein expression in this study, which is consistent with [67]. Gossypol also stimulates LC3-II protein production, as previously demonstrated by [52]. Importantly,

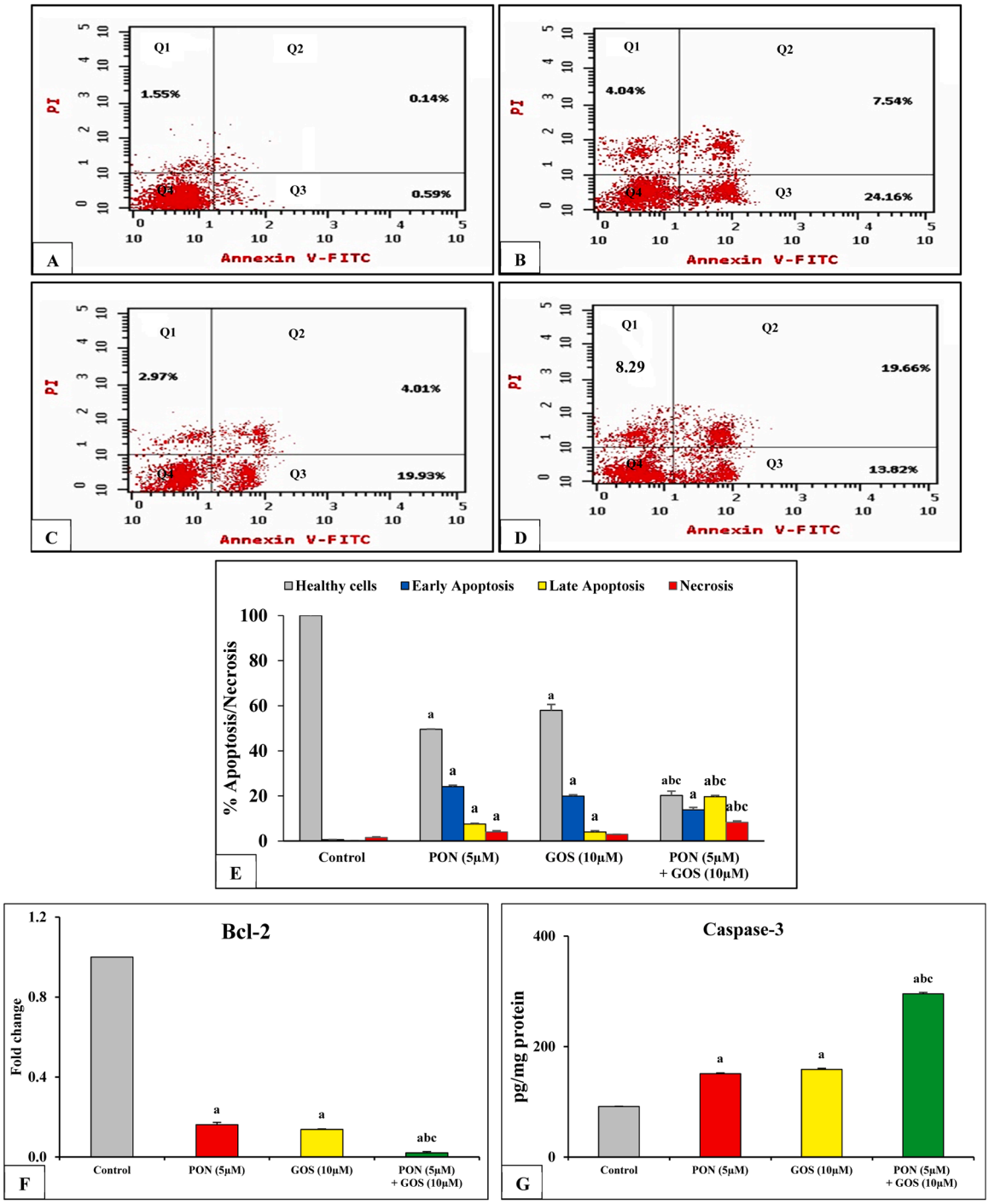

Fig. 6. Gossypol enhances the apoptotic activity of ponatinib in HepG2 cells. Apoptotic cells were determined by PI and Annexin-V staining and analyzed by flow cytometry after 48 h in **(A)** untreated control, **(B)** PON IC_{50}, **(C)** GOS IC_{50}, and **(D)** PON IC_{50} + GOS IC_{50}. **(E)** The X-axis depicts various treatments for HepG2 cells, while the Y-axis reflects the proportion of apoptotic/necrotic cells. **(F, G)** Apoptotic markers such as Bcl-2 and caspase-3 were tested in HepG2 cells after 48 h of treatment. Data are presented as Mean ± SEM (n = 3) and analyzed by one-way ANOVA test followed by a Tukey's *post hoc* test. IC_{50}: the dose of ponatinib and gossypol required to suppress cell growth by 50 % and was determined using nonlinear regression analysis (GraphPad Software Instat, version 5; Inc., La Jolla, CA, USA). PON: ponatinib, GOS: gossypol. $^{a, b, c}$ Significantly different from untreated control, PON and GOS groups, respectively at P <0.05.

ponatinib/gossypol-treated HepG2 cells showed a synergistic increase in LC3-II protein levels compared to either drug alone. Ponatinib had no impact on p62 protein expression, as seen by a non-significant rise, as reported by [67], however gossypol boosted p62 protein expression, as published by [52]. P62 is crucial for autophagy and apoptosis induction [68], activating caspase-8 at the autophagosomal membrane [69], which then activates effector caspases-3, −6, and −7, initiating the extrinsic pathway [70]. The build-up of p62 protein can trigger caspase-3-mediated apoptosis [71] as seen in our study. The addition of gossypol and ponatinib dramatically boosted p62 protein expression compared to either medication alone, displaying that ponatinib/gossypol acts on HepG2 cells via autophagy and apoptotic interaction. Notably, increase of LC3B-II and p62 expression suggests inadequate autophagy [72]. Incomplete autophagy can increase autophagosome production, prevent autophagosome-lysosome fusion, modify lysosome function, and cause cell death [73], a scenario that warrants further

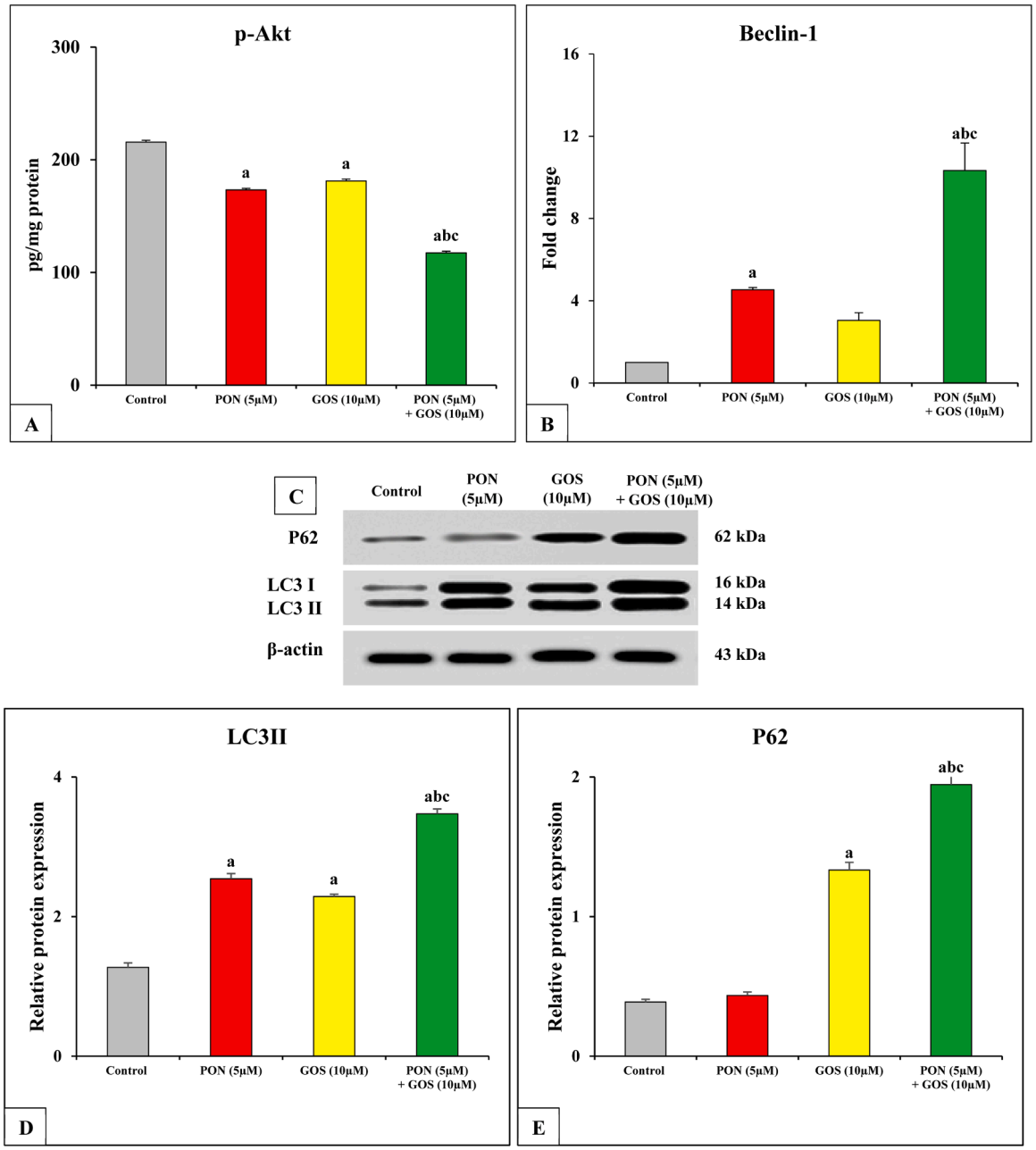

Fig. 7. Autophagic markers p-AKT, beclin-1, LC3II and p62 were evaluated in HepG2 cells after 48 h in untreated control, PON IC_{50}, GOS IC_{50}, and PON IC_{50} + GOS IC_{50}. Data are presented as Mean ± SEM (n = 3) and analyzed by one-way ANOVA test followed by a Tukey's *post hoc* test. IC_{50}: the dose of ponatinib and gossypol required to suppress cell growth by 50 % was determined using nonlinear regression analysis (GraphPad Software Instat, version 5; Inc., La Jolla, CA, USA). PON: ponatinib, GOS: gossypol. [a, b, c] Significantly different from untreated control, PON and GOS groups, respectively at $P < 0.05$.

exploration.

One downside of combination therapy is the increased toxicity on non-cancerous cells [74]. The search for low-toxicity anticancer combination drugs continues to make major strides towards cancer cure. As a result, determining the cytotoxic effect of the ponatinib/gossypol combination on normal cells was crucial. Primary hepatocytes are a useful *in vitro* model for identifying chemicals that may be potentially dangerous for humans [75]. Notably, normal hepatocytes showed minimal harm when ponatinib (% viability 99 −77 %) or gossypol (% viability 99 −76 %) were used separately or in combination (% viability 99 −68 %) at higher concentrations. Interestingly, the 5/10 μM ponatinib/gossypol combination used for the HepG2 cell study settings was safe. For the development of anticancer drugs, selective cytotoxicity is a crucial necessity.

5. Conclusion

Taken together, we discovered for the first time that gossypol (10 μM) may synergistically boost the anticancer activity of ponatinib (5 μM) against HepG2 cells by inhibiting cell growth and increasing ponatinib-induced apoptosis and autophagy via the G0/G1 cell cycle arrest, p-AKT/LC3II/p62, and Bcl2/caspase-3 pathways. This combination, however, had no harm on normal hepatocytes. However, this study's shortcomings include the inability to detect autophagic flux, such as autophagosome maturation and lysosomal degradation. Overall, this combination could be a safe and feasible chemotherapeutic agent for the treatment of HCC patients, a finding that demands additional clinical evaluation.

CRediT authorship contribution statement

Naglaa M. El-Lakkany: Writing – review & editing, Writing – original draft, Visualization, Validation, Supervision, Formal analysis, Conceptualization. **Alaa E. Elsisi:** Visualization, Validation, Supervision, Formal analysis. **Hadeel H. Elkattan:** Writing – original draft, Visualization, Validation, Investigation, Formal analysis, Data curation, Conceptualization.

Declaration of Competing Interest

The authors declare that they have no known competing financial interests or personal relationships that could have appeared to influence the work reported in this paper

Acknowledgements

This research received partial financial support from the Theodor Bilharz Research Institute, Warrak El-Hadar, Imbaba, Giza 12411, Egypt.

Appendix A. Supporting information

Supplementary data associated with this article can be found in the online version at doi:10.1016/j.toxrep.2024.101856.

Data availability

Data will be made available on request.

References

[1] H. Zhang, W. Zhang, L. Jiang, Y. Chen, Recent advances in systemic therapy for hepatocellular carcinoma, 2021 10, Biomark. Res. 10 (1) (2022) 1–21, https://doi.org/10.1186/S40364-021-00350-4.

[2] G.L. Su, O. Altayar, R. O'Shea, R. Shah, B. Estfan, C. Wenzell, S. Sultan, Y. Falck-Ytter, AGA clinical practice guideline on systemic therapy for hepatocellular carcinoma, Gastroenterology 162 (2022) 920–934, https://doi.org/10.1053/j.gastro.2021.12.276.

[3] S. Tu, X. Zhang, D. Luo, Z. Liu, X. Yang, H. Wan, L. Yu, H. Li, F. Wan, Effect of taurine on the proliferation and apoptosis of human hepatocellular carcinoma HepG2 cells, Exp. Ther. Med 10 (2015) 193–200, https://doi.org/10.3892/ETM.2015.2476/HTML.

[4] S.D. Shinde, B. Sahu, A. Chamoli, A. Mandoli, K. Kalia, S.K. Behera, Tyrosine kinases: their role in hepatocellular carcinoma, Thera Precis. Med. Manag. Hepatocell. Carcinoma, Vol. 2: Diagn., Ther. Targets, Mol. Mech. (2022) 133–148, https://doi.org/10.1016/B978-0-323-98807-0.00010-7.

[5] T. Yamaoka, S. Kusumoto, K. Ando, M. Ohba, T. Ohmori, Receptor tyrosine kinase-targeted cancer therapy, Int J. Mol. Sci. 19 (2018), https://doi.org/10.3390/ijms19113491.

[6] S. Crisci, F. Amitrano, M. Saggese, T. Muto, S. Sarno, S. Mele, P. Vitale, G. Ronga, M. Berretta, R. Di Francia, Overview of current targeted anti-cancer drugs for therapy in onco-hematology, Med. (Lith.) 55 (2019), https://doi.org/10.3390/medicina55080414.

[7] Q. Zhou, T. Chen, BI6727, a polo-like kinase 1 inhibitor, synergizes with gefitinib to suppress hepatocellular carcinoma cells via a G2/M arrest mechanism, Pharmazie 77 (2022) 230–235, https://doi.org/10.1691/PH.2022.2392.

[8] A.G. Atanasov, S.B. Zotchev, V.M. Dirsch, I.E. Orhan, M. Banach, J.M. Rollinger, D. Barreca, W. Weckwerth, R. Bauer, E.A. Bayer, M. Majeed, A. Bishayee, V. Bochkov, G.K. Bonn, N. Braidy, F. Bucar, A. Cifuentes, G. D'Onofrio, M. Bodkin, M. Diederich, A.T. Dinkova-Kostova, T. Efferth, K. El Bairi, N. Arkells, T.P. Fan, B. L. Fiebich, M. Freissmuth, M.I. Georgiev, S. Gibbons, K.M. Godfrey, C.W. Gruber, J. Heer, L.A. Huber, E. Ibanez, A. Kijjoa, A.K. Kiss, A. Lu, F.A. Macias, M.J.S. Miller, A. Mocan, R. Müller, F. Nicoletti, G. Perry, V. Pittalà, L. Rastrelli, M. Ristow, G. L. Russo, A.S. Silva, D. Schuster, H. Sheridan, K. Skalicka-Woźniak, L. Skaltsounis, E. Sobarzo-Sánchez, D.S. Bredt, H. Stuppner, A. Sureda, N.T. Tzvetkov, R.A. Vacca, B.B. Aggarwal, M. Battino, F. Giampieri, M. Wink, J.L. Wolfender, J. Xiao, A.W. K. Yeung, G. Lizard, M.A. Popp, M. Heinrich, I. Berindan-Neagoe, M. Stadler, M. Daglia, R. Verpoorte, C.T. Supuran, Natural products in drug discovery: advances and opportunities, 2021 20, Nat. Rev. Drug Discov. 20 (3) (2021) 200–216, https://doi.org/10.1038/s41573-020-00114-z.

[9] S.T. Asma, U. Acaroz, K. Imre, A. Morar, S.R.A. Shah, S.Z. Hussain, D. Arslan-Acaroz, H. Demirbas, Z. Hajrulai-Musliu, F.R. Istanbullugil, A. Soleimanzadeh, D. Morozov, K. Zhu, V. Herman, A. Ayad, C. Athanassiou, S. Ince, Natural products/bioactive compounds as a source of anticancer drugs, Cancers 14 (2022), https://doi.org/10.3390/CANCERS14246203.

[10] S.A.A. Shah, S.S.Ul Hassan, S. Bungau, Y. Si, H. Xu, M.H. Rahman, T. Behl, D. Gitea, F.M. Pavel, R.A.C. Aron, B. Pasca, S. Nemeth, Chemically diverse and biologically active secondary metabolites from marine phylum chlorophyta, 18 (2020) 493, Mar. Drugs 18 (2020) 493, https://doi.org/10.3390/MD18100493.

[11] V.S. Sivasankarapillai, R. Madhu Kumar Nair, A. Rahdar, S. Bungau, D.C. Zaha, L. Aleya, D.M. Tit, Overview of the anticancer activity of withaferin A, an active constituent of the Indian ginseng Withania somnifera, Environ. Sci. Pollut. Res. 27 (2020) 26025–26035, https://doi.org/10.1007/S11356-020-09028-0/FIGURES/3.

[12] K. Mortezaee, M. Najafi, B. Farhood, A. Ahmadi, Y. Potes, D. Shabeeb, A.E. Musa, Modulation of apoptosis by melatonin for improving cancer treatment efficiency: an updated review, Life Sci. 228 (2019) 228–241, https://doi.org/10.1016/J.LFS.2019.05.009.

[13] G. Housman, S. Byler, S. Heerboth, K. Lapinska, M. Longacre, N. Snyder, S. Sarkar, Drug resistance in cancer: an overview, Cancers 6 (2014) 1769–1792, https://doi.org/10.3390/cancers6031769.

[14] N. El-Lakkany, H. Elkattan, A. Elsisi, Ponatinib and gossypol act in synergy to suppress colorectal cancer cells by modulating apoptosis/autophagy crosstalk and inhibiting the FGF19/FGFR4 axis, Asian Pac. J. Trop. Biomed. 13 (2023) 131–138, https://doi.org/10.4103/2221-1691.372286.

[15] N.M. El-Lakkany, H.H. Elkattan, A.E. Elsisi, The ponatinib/gossypol novel combination provides enhanced anticancer activity against murine solid Ehrlich carcinoma via triggering apoptosis and inhibiting proliferation/angiogenesis, Toxicol. Appl. Pharm. 432 (2021) 115767, https://doi.org/10.1016/J.TAAP.2021.115767.

[16] D. Scudiero, R. Shoemaker, K. Paull, A.M.-C. Research, Evaluation of a soluble tetrazolium/formazan assay for cell growth and drug sensitivity in culture using human and other tumor cell lines, U. 1988, AACR 48 (1988) 4827–4833, ⟨https://aacrjournals.org/cancerres/article-abstract/48/17/4827/492702⟩.

[17] T. Chou, Theoretical basis, experimental design, and computerized simulation of synergism and antagonism in drug combination studies, Pharm. Rev. 58 (2006) 621–681, https://doi.org/10.1124/PR.58.3.10.

[18] T.C. Chou, N. Martin, CompuSyn software for drug combinations and for general dose-effect analysis, and user's guide, ComboSyn Inc, Paramus, 2007.

[19] T. -C. Chou, P. Talalay, Generalized equations for the analysis of inhibitions of michaelis-menten and higher-order kinetic systems with two or more mutually exclusive and nonexclusive inhibitors, Eur. J. Biochem 115 (1981) 207–216, https://doi.org/10.1111/j.1432-1033.1981.tb06218.x.

[20] L. Hu, L. Cong, Fibroblast growth factor 19 is correlated with an unfavorable prognosis and promotes progression by activating fibroblast growth factor receptor 4 in advanced-stage serous ovarian cancer, Oncol. Rep. 34 (2015) 2683–2691, https://doi.org/10.3892/or.2015.4212.

[21] B. Wan, Y. Zang, L. Wang, Overexpression of beclin1 inhibits proliferation and promotes apoptosis of human laryngeal squamous carcinoma cell hep-2, Onco Targets Ther. 11 (2018) 3827–3833, https://doi.org/10.2147/OTT.S148869.

[22] C. Song, Y. Han, H. Luo, Z. Qin, Z. Chen, Y. Liu, S. Lu, H. Sun, C. Zhou, HOXA10 induces BCL2 expression, inhibits apoptosis, and promotes cell proliferation in gastric cancer, Cancer Med 8 (2019) 5651–5661, https://doi.org/10.1002/cam4.2440.

[23] K.J. Livak, T.D. Schmittgen, Analysis of relative gene expression data using real-time quantitative PCR and the 2− ΔΔCT method, Methods 25 (2001) 402–408, https://doi.org/10.1006/meth.2001.1262.

[24] C.M. Pfeffer, A.T.K. Singh, Apoptosis: a target for anticancer therapy, Int J. Mol. Sci. 19 (2018), https://doi.org/10.3390/ijms19020448.

[25] M. Brentnall, L. Rodriguez-Menocal, R.L. De Guevara, E. Cepero, L.H. Boise, Caspase-9, caspase-3 and caspase-7 have distinct roles during intrinsic apoptosis, BMC Cell Biol. 14 (2013), https://doi.org/10.1186/1471-2121-14-32.

[26] A. Villanueva, Hepatocellular carcinoma, N. Engl. J. Med 380 (2019) 1450–1462, https://doi.org/10.1056/NEJMRA1713263.

[27] R.S. Zhou, X.W. Wang, Q.F. Sun, Z.J. Ye, J.W. Liu, D.H. Zhou, Y. Tang, Anticancer effects of emodin on HepG2 cell: evidence from bioinformatic analysis, Biomed. Res Int 2019 (2019), https://doi.org/10.1155/2019/3065818.

[28] Y.H.Y.-H.Y.H. Xie, Y.-X.X. Chen, J.-Y.Y. Fang, Comprehensive review of targeted therapy for colorectal cancer, Signal Transduct. Target Ther. 5 (2020) 1–30, https://doi.org/10.1038/s41392-020-0116-z.

[29] J. Jia, F. Zhu, X. Ma, Z.W. Cao, Y.X. Li, Y.Z. Chen, Mechanisms of drug combinations: interaction and network perspectives, Nat. Rev. Drug Discov. 8 (2009) 111–128, https://doi.org/10.1038/NRD2683.

[30] A. Gomes, B. Giri, A. Alam, S. Mukherjee, P. Bhattacharjee, A. Gomes, Anticancer activity of a low immunogenic protein toxin (BMP1) from Indian toad (Bufo melanostictus, Schneider) skin extract, Toxicon 58 (2011) 85–92, https://doi.org/10.1016/J.TOXICON.2011.05.008.

[31] C. Liu, X. Mu, X. Wang, C. Zhang, L. Zhang, B. Yu, G. Sun, Ponatinib inhibits proliferation and induces apoptosis of liver cancer cells, but its efficacy is compromised by its activation on PDK1/Akt/mTOR signaling, Molecules 24 (2019) 1363, https://doi.org/10.3390/molecules24071363.

[32] A.M. Petrilli, J. Garcia, M. Bott, S.K. Plati, C.T. Dinh, O.R. Bracho, D. Yan, B. Zou, R. Mittal, F.F. Telischi, X.Z. Liu, L.S. Chang, D.B. Welling, A.J. Copik, C. Fernández-Valle, Ponatinib promotes a G1 cell-cycle arrest of merlin/NF2-deficient human schwann cells, Oncotarget 8 (2017), https://doi.org/10.18632/ONCOTARGET.15912.

[33] Y. Liu, Y. Ma, Z. Li, Y. Yang, B. Yu, Z. Zhang, G. Wang, Investigation of inhibition effect of gossypol-acetic acid on gastric cancer cells based on a network pharmacology approach and experimental validation, Drug Des. Dev. Ther. 14 (2020) 3615–3623, https://doi.org/10.2147/DDDT.S256566.

[34] Q. Deng, Z. Wang, L. Wang, L. Zhang, X. Xiang, Z. Wang, T. Chong, Lower mRNA and protein expression levels of LC3 and Beclin1, markers of autophagy, were

correlated with progression of renal clear cell carcinoma, Jpn J. Clin. Oncol. 43 (2013) 1261–1268, https://doi.org/10.1093/JJCO/HYT160.
[35] S. Lee, E. Hong, E. Jo, Z.H. Kim, K.J. Yim, S.H. Woo, Y.S. Choi, H.J. Jang, Gossypol induces apoptosis of human pancreatic cancer cells via CHOP/endoplasmic reticulum stress signaling pathway, J. Microbiol. Biotechnol. 32 (2022) 645–656, https://doi.org/10.4014/JMB.2110.10019.
[36] Y. Lu, J. Li, C.E. Dong, J. Huang, H.B. Zhou, W. Wang, Recent advances in gossypol derivatives and analogs: a chemistry and biology view, Https://Doi.Org/10.4155/Fmc-2017-0046 9 (2017) 1243–1275. ⟨https://doi.org/10.4155/FMC-2017-0046⟩.
[37] J. Xiong, J. Li, Q. Yang, J. Wang, T. Su, S. Zhou, Gossypol has anti-cancer effects by dual-targeting MDM2 and VEGF in human breast cancer, Breast Cancer Res. 19 (2017) 27, https://doi.org/10.1186/s13058-017-0818-5.
[38] B.S. Yurekli, B. Karaca, A. Kisim, E. Bozkurt, H. Atmaca, S. Cetinkalp, G. Ozgen, C. Yilmaz, S. Uzunoglu, R. Uslu, F. Saygili, AT-101 acts as anti-proliferative and hormone suppressive agent in mouse pituitary corticotroph tumor cells, J. Endocrinol. Invest 41 (2018) 233–240, https://doi.org/10.1007/s40618-017-0733-8.
[39] C. Inoue, S. Sobue, Y. Kawamoto, Y. Nishizawa, M. Ichihara, A. Abe, F. Hayakawa, M. Suzuki, Y. Nozawa, T. Murate, Involvement of MCL1, c-myc, and cyclin D2 protein degradation in ponatinib-induced cytotoxicity against T315I(+) Ph+ leukemia cells, Biochem Biophys. Res Commun. 525 (2020) 1074–1080, https://doi.org/10.1016/J.BBRC.2020.02.165.
[40] A. Raja, I. Park, F. Haq, S.-M. Ahn, FGF19–FGFR4 signaling in hepatocellular carcinoma, Cells 8 (2019) 536, https://doi.org/10.3390/cells8060536.
[41] T.R. Wilson, M. McEwan, K. McLaughlin, C. Le Clorennec, W.L. Allen, D.A. Fennell, P.G. Johnston, D.B. Longley, Combined inhibition of FLIP and XIAP induces Bax-independent apoptosis in type II colorectal cancer cells, Oncogene 28 (2009) 63–72, https://doi.org/10.1038/onc.2008.366.
[42] R.C. Turkington, D.B. Longley, W.L. Allen, L. Stevenson, K. McLaughlin, P. D. Dunne, J.K. Blayney, M. Salto-Tellez, S. Van Schaeybroeck, P.G. Johnston, Fibroblast growth factor receptor 4 (FGFR4): a targetable regulator of drug resistance in colorectal cancer, Cell Death Dis. 5 (2014) 1–11, https://doi.org/10.1038/cddis.2014.10.
[43] S. Luo, D.C. Rubinsztein, Apoptosis blocks Beclin 1-dependent autophagosome synthesis: an effect rescued by Bcl-xL, Cell Death Differ. 17 (2010) 268–277, https://doi.org/10.1038/cdd.2009.121.
[44] A. Eisenberg-Lerner, S. Bialik, H.U. Simon, A. Kimchi, Life and death partners: apoptosis, autophagy and the cross-talk between them, 2009 16, Cell Death Differ. 16 (7) (2009) 966–975, https://doi.org/10.1038/cdd.2009.33.
[45] S. Zada, J.S. Hwang, M. Ahmed, T.H. Lai, T.M. Pham, O. Elashkar, D.R. Kim, Cross talk between autophagy and oncogenic signaling pathways and implications for cancer therapy, Biochim Biophys. Acta Rev. Cancer 1876 (2021), https://doi.org/10.1016/J.BBCAN.2021.188565.
[46] Y. Wang, H. Zhao, D. Wang, M. Hao, C. Kong, X. Zhao, Y. Gao, J. Li, B. Liu, B. Yang, H. Zhang, J. Jiang, Inhibition of autophagy promoted apoptosis and suppressed growth of hepatocellular carcinoma upon photothermal exposure, J. Biomed. Nanotechnol. 15 (2019) 813–821, https://doi.org/10.1166/JBN.2019.2714.
[47] M. Hashemi, N. Nadafzadeh, M.H. Imani, R. Rajabi, S. Ziaolhagh, S.D. Bayanzadeh, R. Norouzi, R. Rafiei, Z.K. Koohpar, B. Raei, M.A. Zandieh, S. Salimimoghadam, M. Entezari, A. Taheriazam, A. Alexiou, M. Papadakis, S.C. Tan, Targeting and regulation of autophagy in hepatocellular carcinoma: revisiting the molecular interactions and mechanisms for new therapy approaches, 2023 21, Cell Commun. Signal. 21 (1) (2023) 1–22, https://doi.org/10.1186/S12964-023-01053-Z.
[48] H. Wu, X. Che, Q. Zheng, A. Wu, K. Pan, A. Shao, Q. Wu, J. Zhang, Y. Hong, Caspases: a molecular switch node in the crosstalk between autophagy and apoptosis, Int J. Biol. Sci. 10 (2014) 1072, https://doi.org/10.7150/IJBS.9719.
[49] E. Wirawan, L. Vande Walle, K. Kersse, S. Cornelis, S. Claerhout, I. Vanoverberghe, R. Roelandt, R. De Rycke, J. Verspurten, W. Declercq, P. Agostinis, T. Vanden Berghe, S. Lippens, P. Vandenabeele, Caspase-mediated cleavage of Beclin-1 inactivates Beclin-1-induced autophagy and enhances apoptosis by promoting the release of proapoptotic factors from mitochondria, Cell Death Dis. 1 (2010), https://doi.org/10.1038/CDDIS.2009.16.
[50] X. Li, K.Bin Yang, W. Chen, J. Mai, X.Q. Wu, T. Sun, R.Y. Wu, L. Jiao, D.D. Li, J. Ji, H.L. Zhang, Y. Yu, Y.H. Chen, G.K. Feng, R. Deng, J.D. Li, X.F. Zhu, CUL3 (cullin 3)-mediated ubiquitination and degradation of BECN1 (beclin 1) inhibit autophagy and promote tumor progression, Autophagy 17 (2021) 4323–4340, https://doi.org/10.1080/15548627.2021.1912270.
[51] D. Corallo, F. Pastorino, M. Pantile, E. Mariotto, F. Caicci, G. Viola, M. Ponzoni, G. P. Tonini, S. Aveic, Autophagic flux inhibition enhances cytotoxicity of the receptor tyrosine kinase inhibitor ponatinib, J. Exp. Clin. Cancer Res. 39 (2020) 1–16, https://doi.org/10.1186/S13046-020-01692-X/FIGURES/6.
[52] B. Cai, L. Gong, Y. Zhu, L. Kong, X. Ju, X. Li, X. Yang, H. Zhou, Y. Li, Identification of gossypol acetate as an autophagy modulator with potent anti-tumor effect against cancer cells, J. Agric. Food Chem. 70 (2022) 2589–2599, https://doi.org/10.1021/ACS.JAFC.1C06399/SUPPL_FILE/JF1C06399_SI_001.PDF.
[53] A. Thorburn, Apoptosis and autophagy: regulatory connections between two supposedly different processes, Apoptosis 13 (2008) 1–9, https://doi.org/10.1007/S10495-007-0154-9.
[54] B. Levine, S.C. Sinha, G. Kroemer, Bcl-2 family members: dual regulators of apoptosis and autophagy, Autophagy 4 (2008) 600–606, https://doi.org/10.4161/auto.6260.
[55] Q. Liu, D. Zhang, D. Hu, X. Zhou, Y.Z.-M. Immunology, The role of mitochondria in NLRP3 inflammasome activation, U. 2018. , Elsevier, 2018, ⟨https://www.sciencedirect.com/science/article/pii/S0161589018304929?casa_token=Jp4R_7XBVZgAAAAA:aC3PghhQsnUogl3LuUyq4VB42M6OJUuGWQKaN1_9L0gxDhF-H4jQnw5ePdPuQy7HIKmkRHZnaevD⟩. accessed March 31, 2022.
[56] M.B. Menon, S. Dhamija, Beclin 1 phosphorylation - at the center of autophagy regulation, Front Cell Dev. Biol. 6 (2018) 137, https://doi.org/10.3389/fcell.2018.00137.
[57] M. Opydo-Chanek, O. Gonzalo, I. Marzo, Multifaceted anticancer activity of BH3 mimetics: current evidence and future prospects, Biochem Pharm. 136 (2017) 12–23.
[58] J. Lian, X. Wu, F. He, D. Karnak, W. Tang, Y. Meng, D. Xiang, M. Ji, T.S. Lawrence, L. Xu, A natural BH3 mimetic induces autophagy in apoptosis-resistant prostate cancer via modulating Bcl-2–Beclin1 interaction at endoplasmic reticulum, Cell Death Differ. 18 (2011) 60–71, https://doi.org/10.1038/cdd.2010.74.
[59] M. Benvenuto, R. Mattera, J.I. Sticca, P. Rossi, C. Cipriani, M.G. Giganti, A. Volpi, A. Modesti, L. Masuelli, R. Bei, Effect of the BH3 mimetic polyphenol (-)-Gossypol (AT-101) on the in vitro and in vivo growth of malignant mesothelioma, Front Pharm. 9 (2018) 1–13, https://doi.org/10.3389/fphar.2018.01269.
[60] L. Vela, O. Gonzalo, J. Naval, I. Marzo, Direct interaction of Bax and Bak proteins with Bcl-2 homology domain 3 (BH3)-only proteins in living cells revealed by fluorescence complementation, J. Biol. Chem. 288 (2013) 4935–4946.
[61] Y. Cao, D.J. Klionsky, Physiological functions of Atg6/Beclin 1: a unique autophagy-related protein, 2007 17, Cell Res. 17 (10) (2007) 839–849, https://doi.org/10.1038/cr.2007.78.
[62] D.H. Morris, C.K. Yip, Y. Shi, B.T. Chait, Q.J. Wang, Beclin 1-Vps34 complex architecture: Understanding the nuts and bolts of therapeutic targets, 2015 10, Front. Biol. 10 (5) (2015) 398–426, https://doi.org/10.1007/S11515-015-1374-Y.
[63] X. Huang, Q. Qi, X. Hua, X. Li, … W.Z.-O., 2014, Beclin 1, an autophagy-related gene, augments apoptosis in U87 glioblastoma cells, Spandidos-Publications.ComX Huang, Q Qi, X Hua, X Li, W Zhang, H Sun, S Li, X Wang, B LiOncology Reports, 2014•spandidos-Publications.Com 31 (2014) 1761–1767. https://doi.org/10.3892/or.2014.3015..
[64] P. de Medina, J. Bunay, M. Poirot, M. Record, S. Silvente-Poirot, Targeting NR1H/liver X receptor with dendrogenin A differentiates tumor cells to activate a new secretory pathway releasing immunogenic anti-tumor vesicles enriched in LC3-II-associated exosomes, Autophagy 19 (2023) 1036–1038, https://doi.org/10.1080/15548627.2022.2116175.
[65] Y.K. Lee, J.A. Lee, Role of the mammalian ATG8/LC3 family in autophagy: differential and compensatory roles in the spatiotemporal regulation of autophagy, BMB Rep. 49 (2016) 424–430, https://doi.org/10.5483/BMBREP.2016.49.8.081.
[66] W.J. Liu, L. Ye, W.F. Huang, L.J. Guo, Z.G. Xu, H.L. Wu, C. Yang, H.F. Liu, p62 links the autophagy pathway and the ubiqutin-proteasome system upon ubiquitinated protein degradation, Cell Mol. Biol. Lett. 21 (2016), https://doi.org/10.1186/S11658-016-0031-Z.
[67] U.M. Nazim, K. Bishayee, J. Kang, D. Yoo, S.O. Huh, A. Sadra, mTORC1-inhibition potentiating metabolic block by tyrosine kinase inhibitor ponatinib in multiple myeloma, Cancers (Basel) 14 (2022) 2766, https://doi.org/10.3390/CANCERS14112766/S1.
[68] M.A. Islam, M.A. Sooro, P. Zhang, Autophagic regulation of p62 is critical for cancer Therapy, Int J. Mol. Sci. 19 (2018), https://doi.org/10.3390/IJMS19051405.
[69] M.M. Young, Y. Takahashi, O. Khan, S. Park, T. Hori, J. Yun, A.K. Sharma, S. Amin, C.D. Hu, J. Zhang, M. Kester, H.G. Wang, Autophagosomal membrane serves as platform for intracellular death-inducing signaling complex (iDISC)-mediated caspase-8 activation and apoptosis, J. Biol. Chem. 287 (2012) 12455–12468, https://doi.org/10.1074/JBC.M111.309104.
[70] P.C. Ashe, M.D. Berry, Apoptotic signaling cascades, Prog. Neuropsychopharmacol. Biol. Psychiatry 27 (2003) 199–214, https://doi.org/10.1016/S0278-5846(03)00016-2.
[71] C. Zhang, X. Feng, L. He, Y. Zhang, L. Shao, The interrupted effect of autophagic flux and lysosomal function induced by graphene oxide in p62-dependent apoptosis of F98 cells, J. Nanobiotechnol. 18 (2020) 1–17, https://doi.org/10.1186/S12951-020-00605-6/FIGURES/7.
[72] H.L. Hsu, B.J. Lin, Y.C. Lin, C.C. Tu, N.L. Nguyen, C.C. Wang, M.C. Chen, C. H. Chen, Cucurbitacin E exerts anti-proliferative activity via promoting p62-dependent apoptosis in human non-small-cell lung cancer A549 cells, Curr. Issues Mol. Biol. 45 (2023) 8138–8151, https://doi.org/10.3390/CIMB45100514/S1.
[73] Q. Zhang, S. Cao, F. Qiu, N. Kang, Incomplete autophagy: trouble is a friend, Med Res Rev. 42 (2022) 1545–1587, https://doi.org/10.1002/MED.21884.
[74] R.B. Mokhtari, T.S. Homayouni, N. Baluch, E. Morgatskaya, S. Kumar, B. Das, H. Yeger, Combination therapy in combating cancer, Oncotarget 8 (2017) 38022–38043, https://doi.org/10.18632/ONCOTARGET.16723.
[75] S. Wilkening, A. Bader, Influence of culture time on the expression of drug-metabolizing enzymes in primary human hepatocytes and hepatoma cell line HepG2, J. Biochem Mol. Toxicol. 17 (2003) 207–213, https://doi.org/10.1002/JBT.10085.